

Materializing Quantum Effects: Dark Mater

Eduardo V. Flores¹
Department of Physics & Astronomy
Rowan University
Glassboro, NJ 08028

Quantum effects that materialize always fulfill the conservation laws and principles of physics. Physical interactions require the presence of sources and vehicles of conserved quantities. Generally, on-shell particles are sources, and off-shell particles are vehicles of conserved quantities. We have found that when either the source or vehicle is missing, quantum effects cannot materialize. Our findings resolve the alleged violation of complementarity in the Afshar experiment. Additionally, our findings indicate that galactic neutrinos should be treated as a classical ideal gas. To this end, we present a simplified model of a classical ideal gas of neutrinos that accounts for effects attributed to dark matter to a reasonable degree of approximation.

Keywords: Conservation laws, complementarity principle, Afshar experiment, neutrinos, quantum gravity, particle-antiparticle symmetry

Introduction

The accuracy of the Dirac equation in predicting the behavior of the hydrogen atom is due to the significant difference in mass between the electron and proton [1]. The heavy proton is hardly affected by the motion of the electron. In cases where the masses of bound state particles are comparable, such as in positronium, a perturbation to the Dirac equation is the approach that reproduces experimental results [2,3]. These perturbations result in small energy-momentum transfers that have been identified as off-shell particles. Particles come in two energy-momentum states, on-shell and off-shell [4]. On-shell particles satisfy the energy-momentum relation for free particles, $E^2 = p^2 c^2 + m^2 c^4$, and could propagate to infinity. Off-shell particles, also known as virtual particles, do not satisfy this relation and cannot be set free. Off-shell particles exist only briefly and may have a limited range. They have peculiar properties, including the ability to transfer energy-momentum as well as discrete units of angular momentum and charge between interacting particles. Interactions mediated by off-shell particles obey conservation laws. Interestingly, even though the charm quark has a heavier mass than a proton, off-shell charm quarks can appear within a proton [5].

The basic interaction in quantum electrodynamics is described by the Feynman diagram in Fig. 1a; all other interactions are built from this one [1]. For instance, the interaction of light with light described by the diagram in Fig. 1b, requires four basic interactions. The interaction in Fig. 1b gives rise to non-linear electrodynamics summarized by Euler-Heisenberg effective lagrangian [6,7]. Bound states can also be describe using the basic interaction in Fig. 1a infinitely many times; thus, the resulting Feynman diagram has the form of an infinite ladder [3]. In hydrogen, subtle effects like the Lamb's shift can only be explained by the exchange of off-shell particles [1].

¹ Email: flores@rowan.edu

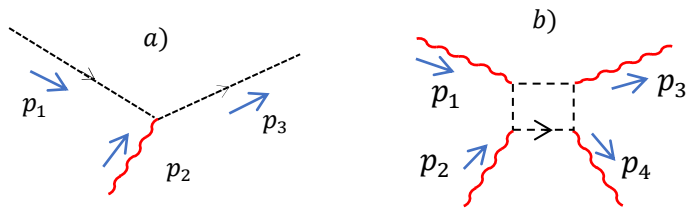


Fig. 1 Feynman diagrams in quantum electrodynamics. a) An electron interacts with a photon. This interaction gives rise to all other interactions in quantum electrodynamics. b) Light interacts with light. Two photons interact with an off-shell electron in a closed loop and two new photons emerge. This photon-photon interaction gives rise to non-linear electrodynamics.

Let's consider the electron in hydrogen with quantum numbers $n = 4, l = 1$, and $m = 0$. In this state, the electron's radial probability density displays a pattern with alternating high and low-intensity regions. This pattern is formed as the electron is driven by off-shell particles from low-intensity regions to high-intensity regions. These regions of high and low intensity are similar to the bright and dark fringes observed in interference patterns of light. We propose that a photon is also driven by off-shell particles from low to high-intensity regions in the formation of an interference pattern on a screen. The basic process is described by a Feynman diagram similar to the one shown in Fig. 1b. An incoming photon with momentum \vec{p}_1 interacts with an off-shell electron in a closed loop. The two photon lines with momentum \vec{p}_2 and \vec{p}_4 represent the Coulomb field of a charge that belongs to the screen. The outgoing photon emerges with momentum \vec{p}_3 . This process, known as Delbruck scattering, is actually very weak for visible light [8-11]. Therefore, similar to bound states, it would take an infinite number of these weak interactions to produce the observed results. T. Lee proposes a similar mechanism to explain the unusual deviations of x-ray photons by a Coulomb field [12,13].

Particle-wave duality

Which-way information, K , is a particle property, and visibility, V , is a wave property. Both of these values are limited by Bohr's principle of complementarity, which is expressed by the inequality [14-16]:

$$K^2 + V^2 \leq 1. \quad (1)$$

Inspired by Wheeler's work, we can associate the which-way information, K , with our ability to identify the origin of a particle by applying the principle of momentum conservation [14]. By detecting the final position and direction of a free particle, we can deduce where it originated. When we can accurately determine the particle's origin, we have maximum which-way information, $K = 1$. If we cannot identify the particle's origin, we have zero which-way information, $K = 0$. Additionally, we can have partial which-way information, $1 > K > 0$.

On the other hand, visibility, V , measures the contrast between bright and dark fringes in an interference pattern formed by the accumulation of particles. If a particle avoids a particular region and is attracted to an adjacent region, it contributes to the formation of adjacent dark and bright fringes, and its visibility is maximum, $V = 1$. If a particle is equally likely to reach any point within a region, it contributes to the formation of a uniform distribution, and its visibility is zero, $V = 0$. We can also have partial visibility, $1 > V > 0$.

Consider two laser beams, in phase, that cross at a small angle, then separate and ultimately end up at detectors, as depicted in Figure 2. The experiment could be conducted at a low photon count, such that there is a high probability of there being only one photon present in the entire setup at any given time. The experiment could be carried out with single electrons and, due to matter-radiation symmetry, it would be unexpected if the results were different to the photon case.

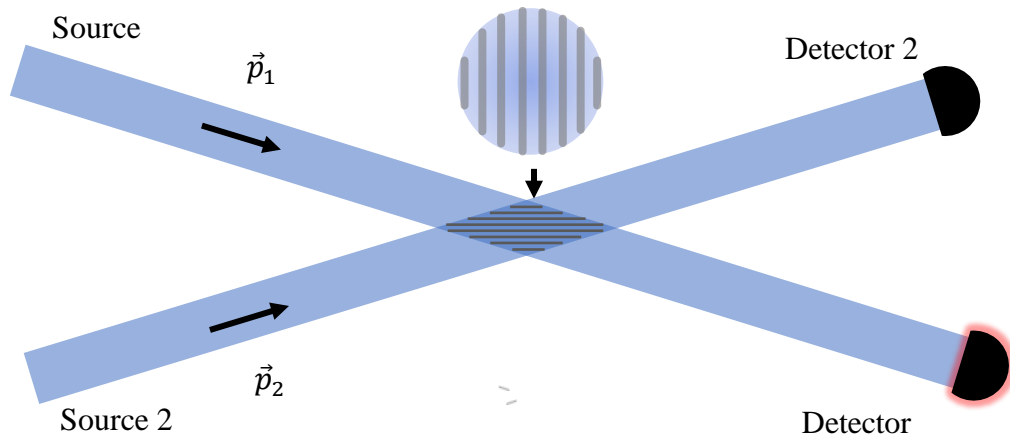


Fig. 2 Two coherent beams intersect and end at detectors. Two low intensity laser beams in phase intersect and ultimately end up at detectors. When detector 1 clicks, we can infer with certainty that the photon came from source 1 and the which-way information is 1. At the intersection of the beams, the electric field undergoes both constructive and destructive interference, resulting in a characteristic pattern with fringes.

When two plane waves, which are in phase, intersect at a small angle α , they produce an electric field intensity of $E_0^2(1 + \cos[2\pi\alpha y/\lambda])$, where y represents the transverse location and λ is the wavelength [17]. Therefore, in the experiment depicted in Fig. 2, the electric field exhibits constructive and destructive interference fringes at the region where the beams intersect. Interestingly, if we were to insert an opaque screen at the intersection of the beams, we would observe interference fringes with maximum visibility ($V = 1$) as seen in the circle in Fig. 2. Similarly, the net wavefunction of two electron plane waves under equivalent conditions would display similar interference fringes.

Consider the case when there is a high probability that there is only one photon in the entire setup in Fig. 2. The linear momentum of the photon should be constant from source to detector. However, the field momentum, which is proportional to the electric field intensity, changes from uniform before and after the beams cross, to one with high and low intensity regions at the beam intersection as seen in Fig. 2. When the photon crosses the beam intersection, its momentum would experience predetermined deflections if it were to follow the field momentum distribution. However, these predetermined changes in the momentum of a free particle violate momentum conservation. We conclude that the electromagnetic field momentum distribution is virtual in the sense that the free photon cannot fulfill it.

Similarly, in an experiment with electrons, when a single electron is present in the entire setup and the beams cross freely, we expect the electron's momentum to be constant from source to detector. The electron, like the photon, must ignore the interference fringes in its wavefunction at the beam intersection. In both

cases, the interference fringes are virtual as they cannot be materialized because there is no external source to provide the necessary momentum for deflections.

The Afshar experiment

Using the setup in Figure 2, the authors of the experiment in Ref. 18 aimed to measure both the visibility and which-way information simultaneously [18]. To accomplish this, they employed a technique originally introduced by S. S. Afshar [19]. In this technique, a dark wire that is 12.5 times thinner than the distance between consecutive bright or dark fringes is scanned across the intersection region of the beams. First, they consider the case where the beams cross freely and establish the photon count at the end detectors. Next, under similar conditions, the 17 μm thick wire is scanned across the beam intersection. The ratio (f) of the photon count with the wire in place over the photon count without the wire is plotted in Figure 3. The solid line represents a calculation of f using Fraunhofer diffraction [18v2]. Remarkably, the theoretical and experimental results are in excellent agreement.

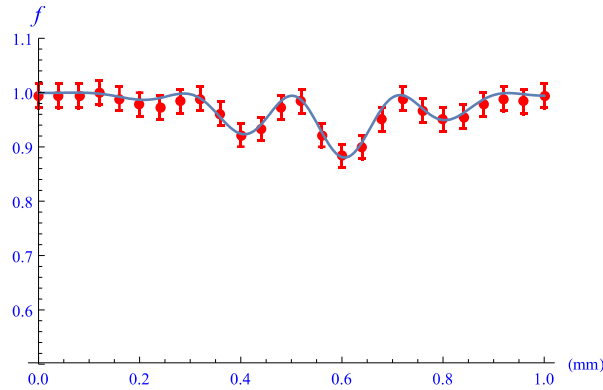


Fig. 3 Fraction of photon count (f) at end detector. This plot displays the fraction of photon count at one of the end detectors as a 17 μm thick wire is scanned across the 1.0 mm beam intersection. The error bars in the plot represent statistical uncertainties, while the solid line represents the theoretical prediction using Fraunhofer diffraction. Remarkably, there is evidence that these results do not change even when the experiment is conducted at an average separation between one photon and the next of 3 km [18].

By analyzing Figure 3, it can be observed that the fraction of photon count decreases to 0.88 when the 17 μm thick wire is positioned at 0.6 mm, suggesting the existence of a bright fringe at this location. This reduction in the photon count corresponds to a 12% decrease in the total number of photons absorbed and scattered by the wire. Conversely, when the wire is placed at 0.72 mm, the fraction of photon count remains close to one, indicating that no photon losses occur at this position. These observations indicate that the wire thickness significantly affects the photon count, and the position of the wire can be used to determine the presence or absence of interference fringes.

In classical physics, the interference pattern in the electromagnetic is materialized regardless of whether we measure it or not. Thus, when the wire is placed at 0.72 mm, at the center of a dark fringe, there are no losses due to wire diffraction because there is no field to diffract; thus, the which-way information is maintained ($K \approx 1$). Photons that come from source 1 (2) will most likely end up at detector 1 (2). Since there are no photons at the wire, photon intensity at the wire is zero ($I_0 \approx 0$). Photons must be found in a

nearby region where the intensity is nonzero ($I \neq 0$). As a result, the visibility is 1 ($V = \frac{I-I_0}{I+I_0} \approx 1$). Thus, the complementarity inequality in Eq. 1 is violated, as $K^2 + V^2 \approx 2$.

Similarly, in the Afshar experiment [19], comparable results were obtained. However, instead of a single wire, a wire grid was used. It is worth noting that some authors have claimed to have resolved the paradoxical results of the Afshar experiment using grid diffraction analysis [20,21]. Nevertheless, we contend that grid diffraction analysis does not solve the paradox of Afshar's experiment for reasons similar to those of single-wire diffraction analysis [22,23].

Resolution of the paradox

We find that if an interference pattern were to be materialized at the beam intersection in Fig. 2, with or without the presence of a wire as in classical physics, the complementarity principle and momentum conservation could be violated. Since these principles cannot be violated, we propose that the presence of the wire materializes the interference pattern at its location. Quantum electrodynamics provides the mechanism for this materialization. As a photon approaches the wire, it interacts through off-shell particles with the approximately 10^{13} charges that make up the wire. These off-shell particles deflect the photon away from regions with low electric field intensity and move it towards regions with high electric field intensity. In Fig. 2 and Fig. 5, the high-intensity regions are found at the two beams and at the bright fringes at the beam intersection, while the low-intensity regions are only found at the dark fringes at the beam intersection.

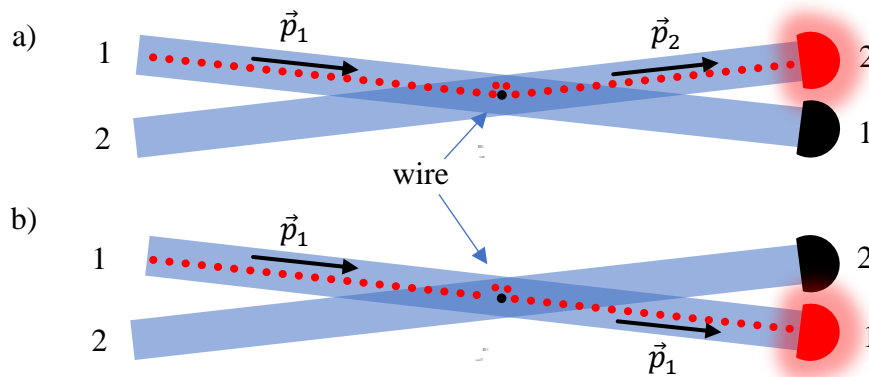


Fig. 5 Photon and a wire at the center of a dark fringe. Assuming a photon is emitted from source 1 and initially heads towards the wire, located at the center of a dark fringe, it is then deflected around the wire, contributing to the formation of a dark fringe and achieving a high level of visibility, $V = 1$. Beyond the wire, the photon encounters two identical regions of high electric field, which leads to two equally likely possibilities: a) the photon takes momentum \vec{p}_2 and enters beam 2, or b) the photon takes momentum \vec{p}_1 and enters beam 1. When a detector registers the photon, it is impossible to determine which source it originated from, resulting in zero which-way information, $K = 0$. The wire provides the necessary momentum for these deflection maneuvers, which is transferred by off-shell particles.

When a photon approaches the wire and is deflected around it, it can achieve maximum visibility, $V = 1$, as it contributes to the formation of adjacent dark and bright fringes. After the deflection, the photon encounters two outgoing beams with identical electric field intensity. Due to the random nature of quantum

mechanics, the photon is randomly directed into one of the beams. This randomness erases the which-way information, $K = 0$, as momentum conservation cannot reveal whether the photon originated from source 1 or 2. This mechanism ensures that the photon count at the end detectors remains unchanged, as observed in the experiment. At the wire, the visibility is 1, while the which-way information is 0. As a result, the complementarity inequality in Eq. 1 is preserved.

Galactic Neutrinos

Air in standard atmospheric conditions is treated as a classical ideal gas. We note that there are approximately 2.5×10^{19} air molecules in a cubic centimeter of air, with an effective radius of about 2.0×10^{-10} m per molecule. If galactic neutrinos with an average mass of $0.5 \text{ eV}/c^2$ [24] were to constitute dark matter, their density at the solar system would be 6.24×10^8 neutrinos per cubic centimeter [25]. However, due to the short range of the weak interaction, neutrinos can only interact with each other up to distances of the order of 10^{-18} m. These numbers suggest that galactic neutrinos are too far from each other to exchange off-shell vector bosons. Thus, quantum effects such as fermionic repulsion cannot be materialized. Therefore, we may treat galactic neutrinos as a classical ideal gas with negligible viscosity.

To study a classical ideal gas, we start with Euler's equation of motion along a streamline for inviscid compressible flows

$$\frac{\partial \vec{v}}{\partial t} + (\vec{v} \cdot \vec{\nabla}) \vec{v} + \frac{\vec{\nabla} P}{\rho} - \vec{g} = 0, \quad (2)$$

where P is pressure, ρ is density, \vec{v} is velocity and \vec{g} is the gravitational field. Here we consider the equilibrium state, $\vec{v} = 0$. Since we assume spherical symmetry gravity points inwards along the radial direction. Euler's equation reduces to

$$\frac{1}{\rho} \frac{\partial P}{\partial r} + g = 0. \quad (3)$$

We assume that galactic neutrinos obey the ideal gas law, $P = \frac{k_B T}{m} \rho$, where m is the average neutrino mass, and we assume thermal equilibrium for simplicity. In this introductory model, regular mass is only found within r_0 , the location of the Solar system, while dark matter is present both inside and outside of r_0 . Our goal is to produce a rotational curve outside of r_0 .

The gravitational field $g(r)$ is generated by a central mass, M_0 , inside r_0 , plus dark matter outside r_0 ,

$$g(r) = G \frac{M_0 + 4\pi \int_{r_0}^r \rho(y) y^2 dy}{r^2}. \quad (4)$$

Equation 3 is now an integrodifferential equation

$$\frac{k_B T}{4\pi m G} \frac{r^2}{\rho} \frac{\partial \rho}{\partial r} + \frac{M_0}{4\pi} + \int_{r_0}^r \rho(y) y^2 dy = 0. \quad (5)$$

Given M_0 and dark matter density $\rho(r_0)$ at r_0 this equation can be solved numerically once a value for the T/m is chosen. Once we obtain the density $\rho(r)$, we calculate $g(r)$ in Eq. 4. Using Newton's laws, $m_s g = m_s \frac{v^2}{r}$, we obtain the rotational curve, $v(r) = \sqrt{gr}$, for a satellite with mass m_s in circular orbit around the galaxy,

$$v(r) = G \sqrt{\frac{M_0 + 4\pi \int_{r_0}^r \rho(y) y^2 dy}{r}}. \quad (6)$$

The plot in Fig. 6 shows the rotational curve for the Milky Way galaxy. The theoretical curve corresponds to a ratio of $\frac{T}{m} = 6$, where T is the temperature and m is the average neutrino mass, in units such that when the neutrino mass is 0.89×10^{-36} kg or 0.5 eV/ c^2 [24], the corresponding gas temperature is 5.35 mK. At the Solar system, $r_0 = 8.34$ kpc, the dark matter density is $\rho(r_0) = 0.01 M_\odot/\text{pc}^3$ [25].

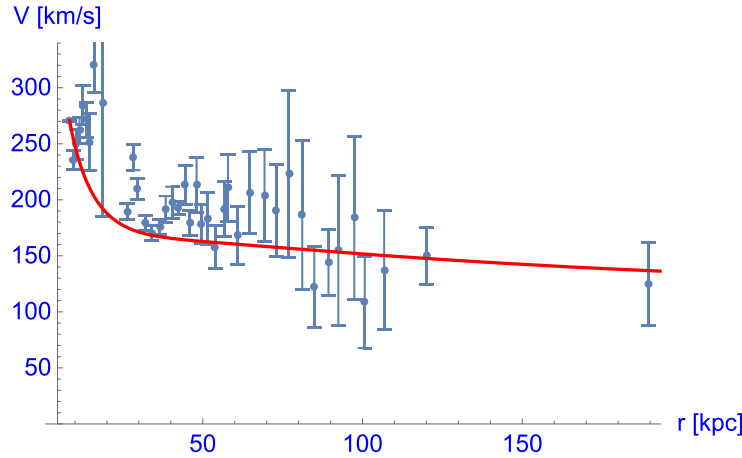


Fig. 6 Rotational curve for the Milky Way beyond the Solar system. Assuming spherical symmetry, dark matter density at the Solar system of $0.01 M_\odot/\text{pc}^3$ and no ordinary mass beyond the Solar system, we predict a rotational curve that roughly fits the observed rotational curve. The only free parameter here is gas temperature over neutrino mass ratio, T/m .

Among the features of ideal gases is isentropic wave propagation like sound waves in air. At the Milky Way galaxy, the isentropic wave speed is $v_s = \sqrt{\frac{\gamma k_B T}{m}} = 370$ km/s, where $\gamma = 5/3$ for a gas with 3 degrees of freedom.

The recent gravitational lensing observations suggest that there are large density fluctuations in dark matter caused by the quantum interference between dark matter axions, which manifest as waves [26]. We note that the classical ideal neutrino gas must also be sensitive to gravitational perturbations due to its very low mass. The movement of ordinary matter would significantly affect the density of the neutrino gas. It is probable that galactic neutrinos undergo similar fluctuations to those of weather in the atmosphere. It would be crucial to investigate whether the random density fluctuations of galactic neutrinos could explain the observed deviations in gravitational lensing [26].

Concluding remarks

According to classical physics, a dark fringe should appear at the location of a wire when two beams meet, regardless of the presence of the wire. However, quantum mechanics tells us that the wire's presence is necessary for the dark fringe to materialize. Photons exchange energy-momentum with the wire through an

interaction mediated by off-shell particles, which deflects the photons that would otherwise hit the wire. These photons gain full visibility ($V = 1$) as they form a dark fringe. After passing the wire, the photons are given a precise momentum that randomly directs them into one of the two outgoing beams. This random process destroys which-way information ($K = 0$) and preserves complementarity in the Afshar experiment. We note that randomness is a typical quantum mechanical property.

It is worth noting that the wavefunction for Dirac neutrinos orbiting the galaxy is determined by the Dirac equation in curved spacetime. However, for a neutrino to manifest the effects of its wavefunction, it would require the presence of off-shell particles to transfer the necessary energy-momentum, much like an electron in a hydrogen atom. The only long-range interaction of neutrinos in the galaxy is gravitational. Based on the observations presented in this paper, if a neutrino in a galaxy materializes the effects of its wavefunction, it would provide evidence that the exchange of off-shell gravitons is responsible for gravitational interaction, which are hypothetical particles at present. Therefore, if galactic neutrinos follow their wavefunction, it would indicate that gravity is a quantum force. However, if galactic neutrinos behave as a classical ideal gas, then gravity would be a distortion of spacetime, as predicted by general relativity. It is important to note that if galactic neutrinos follow their wavefunction, they would obey Fermi-Dirac statistics and, thus, would not be strong dark matter candidates [27].

It would be a boost to the Standard Model of particles if galactic neutrinos happen to be dark matter. It is conceivable that low energy neutrinos and antineutrinos would be in equilibrium as annihilation can only result in the same type of pair. We note that there could be sufficient excess of antineutrinos to restore the particle-antiparticle symmetry in the universe.

Acknowledgments

We wish to thank Michael Lim, whose comments sparked the insight necessary for this work

References

- 1 J. D. Bjorken & S. D. Drell, *Relativistic Quantum Mechanics* (McGraw-Hill, New York, 1964).
- 2 H. Bethe, E. Salpeter, "A Relativistic Equation for Bound-State Problems". *Phys. Rev.* 84 (6): 1232 (1951)
- 3 W. Greiner and J. Reinhardt, *Quantum Electrodynamics* (Springer, 2009), Fourth Edition.
- 4 M. J. G. Veltman, *Facts and Mysteries in Elementary Particle Physics* (World Scientific Publishing Co. Pte. Ltd., 2003), p. 254
- 5 R. D. Ball, et al., *Nature*, 608, pages483–487 (2022)
- 6 W. Heisenberg and H. Euler, *Z. Phys.* 98, 714 (1936), arXiv:physics/0605038 [physics].
- 7 J. S. Schwinger, *Phys. Rev.* 82, 664 (1951), [,116(1951)].
- 8 M. Delbruck, *Zeits. Phys.*, 84, 144 (1933)
- 9 R. Karplus & M. Neuman, *Phys. Rev.* 83, 776 (1951).
- 10 V. Costantini, B. De Tollis and G. Pistoni, *Nuovo Cimento*, 2, 733 (1971)
- 11 Delbruck observation reference here: M. Schumacher, I. Borchert, F. Smend, and P. Rullhusen, *Phys. Lett.* 59B, 134 (1975).
- 12 J. Y. Kim & T. Lee, *Mod. Phys. Lett. A*, Vol. 26, No. 20 (2011) pp. 1481-1485 arXiv:1012.1134v2
- 13 T. Lee, arXiv:1711.00160v2 (2018)
- 14 J. A. Wheeler, in *Quantum Theory and Measurement* (Princeton University Press, 1983).
- 15 D. Greenberger and A. Yasin, *Phys. Lett. A* 128, 391 (1988).

- 16 B.-G. Englert, Phys. Rev. Lett. 77 2154 (1996).
- 17 R. Buonpastore, E. Knoesel and E. Flores, Optik 121, 1009-10012 (20010)
- 18 E. V. Flores, J. Scaturro, arXiv:1412.1077v4
- 19 S. S. Afshar, E. V. Flores, K. F. McDonald, E. Knoesel, Found. Phys., 37 (2) 295-305 (2007)
- 20 Steuernagel, O., Found. Phys. 37, 37: 1370–1385 (2007)
- 21 V. Jacques, N. D. Lai, A. Dreau, D. Zheng, D. Chauvat, F. Treussart, P. Grangier, J-F Roch, New J. Phys. 10, 123009 (2008)
- 22 E. Flores, Found. Phys. 38, 778- 781 (2008)
- 23 E. Flores and J. M. De Tata, Found. Phys. 40, 1731–1743 (2010)
- 24 The KATRIN Collaboration. Nat. Phys. 18, 160–166 (2022).
- 25 J. I. Read, The Local Dark Matter Density, arXiv:1404.1938v2
- 26 Amruth, A., Broadhurst, T., Lim, J. et al. Einstein rings modulated by wavelike dark matter from anomalies in gravitationally lensed images. Nat Astron (2023).
- 27 S. Tremaine and J. E. Gunn, Phys. Rev. Lett. 42, 407